


# Crystal Structure of Bovine Alpha-Chymotrypsin in Space Group P6<sub>5</sub>

Andrew C. Marshall <sup>1</sup>, Benjamin G. Keiller <sup>2</sup>, Jordan L. Pederick <sup>1</sup>, Andrew D. Abell <sup>3</sup> and John B. Bruning <sup>1,\*</sup> 

<sup>1</sup> Institute for Photonics and Advanced Sensing (IPAS), School of Biological Sciences, The University of Adelaide, Adelaide 5005, Australia; andrew.c.marshall@adelaide.edu.au (A.C.M.); jordan.pederick@adelaide.edu.au (J.L.P.)

<sup>2</sup> School of Agriculture, Food and Wine, Department of Plant Science, The University of Adelaide, Adelaide 5005, Australia; benjamin.keiller@adelaide.edu.au

<sup>3</sup> Institute for Photonics and Advanced Sensing (IPAS), Department of Chemistry, and the Centre for Nanoscale BioPhotonics, The University of Adelaide, Adelaide 5005, Australia; andrew.abell@adelaide.edu.au

\* Correspondence: john.bruning@adelaide.edu.au

Received: 21 November 2018; Accepted: 7 December 2018; Published: 10 December 2018



**Abstract:** Chymotrypsin is a protease that is commonly used as a standard for protein crystallization and as a model system for studying serine proteases. Unliganded bovine  $\alpha$ -chymotrypsin was crystallized at neutral pH using ammonium sulphate as the precipitant, resulting in crystals that conform to P6<sub>5</sub> symmetry with unit cell parameters that have not been reported previously. Inspection of crystallographic interfaces revealed that the major interface between any two molecules in the crystal lattice represents the interface of the biological dimer, as previously observed for crystals of unliganded  $\alpha$ -chymotrypsin grown at low pH in space group P2<sub>1</sub>.

**Keywords:** trypsin-like serine protease; endopeptidase; hydrolase

## 1. Introduction

Chymotrypsin is a serine endopeptidase secreted from the pancreas, and it is involved in proteolytic digestion. Chymotrypsinogen A is activated via hydrolysis of the Arg15-Ile16 peptide bond by trypsin to produce  $\pi$ -chymotrypsin. Autolytic cleavage of  $\pi$ -chymotrypsin at peptide bonds 13-14, 146-147, and 148-149 then follows to produce  $\alpha$ -chymotrypsin, which consists of three separate polypeptides cross-linked by five disulphide bonds [1]. Chymotrypsin was one of the first protein structures solved by X-ray crystallography, and was the first solved structure of a protease [2]. Researchers quickly discovered that chymotrypsin can easily be crystallized using ammonium sulphate as a precipitant, often with lower pH (<4.5), leading to crystal forms conforming to the space group P2<sub>1</sub>, while at higher pH (>4.5), crystal forms usually conform to the space group P4<sub>2</sub>2<sub>1</sub>2, with the latter crystal form primarily used for crystallization with a ligand. Since this discovery, a number of other crystal forms have been reported. A summary of representative published crystal forms is presented in Table S1. Given its long history of study and ease of purification, chymotrypsin has been used as a model system for several purposes. Chymotrypsin is often used in combination with other proteins as a control to study protein crystallization itself, such as probing general crystallization techniques as well as general seeding techniques. In addition, many other proteases, such as the proteasome, elastases, cathepsins, and calpain, have proven difficult to study in vitro due to problems in purification. As such, chymotrypsin is often used as a model for studying ligand-protease interactions, especially with regard to structure-guided drug design [3–5]. Here, we report a previously undocumented crystal form

of  $\alpha$ -chymotrypsin (Table 1) solved by X-ray crystallography to a resolution of 1.86 Å in the space group P6<sub>5</sub>.

**Table 1.** Macromolecule information.

| Source Organism  | <i>Bos taurus</i>   |
|--|---|
| Complete amino acid sequence of chymotrypsinogen A (UniProt: P00766) | CGVPAIQPVL SGLSRIVNGE EAVPGSWPWQ VSLQDKTGFH FCGGSLINEN<br>WVVTAAHCGV TTSDVVVAGE FDQGSSEKI QKLKIAKVKF NSKYNSLTIN<br>NDITLLKLST AASFSQTVSA VCLPSASDDF AAGTTCVTTG WGLTRYTNAN<br>TPDRLQQASL PLLSNTNCKK YWGTKIKDAM ICAGASGVSS CMGDSGGPLV<br>CKKNGAWTLV GIVSWGSSSTC STSTPGVYAR VTALVNWWQQ TLAAN |

## 2. Materials and Methods

### 2.1. Macromolecule Production

TLCK (Tosyl-L-lysyl-chloromethane hydrochloride)-treated  $\alpha$ -chymotrypsin A isolated from bovine pancreas was purchased from Worthington Biochemical Corporation (Lakewood, NJ, USA) as a dialyzed (1 mM HCl), lyophilized powder (product code: CDTLCK) and dissolved in 0.1 M HEPES pH 7.0 to a final concentration of 20 mg/ml.

Amino acids 14, 15, 147, and 148 (underlined) were removed during processing of chymotrypsinogen A to produce  $\alpha$ -chymotrypsin.

### 2.2. Crystallization

Protein was crystallized by vapour-diffusion using the hanging drop method at 16 °C. Crystals formed as rods with a maximum dimension of approximately 400 µm after 1 month with 2 M ammonium sulphate as the reservoir solution. Complete details of the crystallization conditions are given in Table 2. Prior to data collection, crystals were cryoprotected in Paratone-N (Hampton Research) and flash cooled in liquid nitrogen.

**Table 2.** Crystallization.

| Method                                 | Vapour Diffusion, Hanging Drop   |
|--|--|
| Plate type                             | 24-well tissue culture plate with glass cover slips sealed using vacuum grease |
| Temperature (K)                        | 289  |
| Protein concentration                  | 20 mg/mL   |
| Buffer composition of protein solution | 0.1 M HEPES pH 7.0   |
| Composition of reservoir solution      | 2 M (NH <sub>4</sub> ) <sub>2</sub> SO <sub>4</sub>                            |
| Volume and ratio of drop               | 2 µL drop volume with 1:1 ratio of protein solution to reservoir solution      |
| Volume of reservoir                    | 0.5 mL   |

### 2.3. Data Collection and Processing

X-ray diffraction data were collected at 13000 eV from a single crystal using the MX1 beamline [6] at the Australian Synchrotron. A total of 179 frames were collected at 1° intervals with 1° oscillation. Data were processed using iMosflm (CCP4i, Oxford, UK) [7]. Data collection and processing statistics are shown in Table 3.

**Table 3.** Data collection and processing. Values for the outer shell are given in parentheses. All data were collected from a single crystal.

| Diffraction Source             | Australian Synchrotron Beamline MX1 |
|--------------------------------|-------------------------------------|
| Wavelength (Å)                 | 0.9537                              |
| Temperature (K)                | 100                                 |
| Detector                       | ADSC quantum 210r CCD               |
| Crystal-detector distance (mm) | 184.95                              |

Table 3. Cont.

| Diffraction Source   | Australian Synchrotron Beamline MX1 |
|--|-------------------------------------|
| Rotation range per image (°)                               | 1                                   |
| Total rotation range (°)                                   | 179                                 |
| Exposure time per image (s)                                | 1                                   |
| Space group  | P6 <sub>5</sub>                     |
| <i>a</i> , <i>b</i> , <i>c</i> (Å)                         | 126.8, 126.8, 122.0                 |
| $\alpha$ , $\beta$ , $\gamma$ (°)                          | 90, 90, 120                         |
| Mosaicity (°)  | 0.53                                |
| Resolution range (Å)                                       | 29.55–1.86 (1.89–1.86)              |
| Total No. of reflections                                   | 868057 (31308)                      |
| No. of unique reflections                                  | 93385 (4606)                        |
| Completeness (%)   | 100.0 (99.7)                        |
| Redundancy   | 9.3 (6.8)                           |
| $\langle I/\sigma(I) \rangle$                              | 12.2 (1.0 <sup>†</sup> )            |
| CC <sub>1/2</sub>  | 0.998 (0.383)                       |
| <i>R</i> <sub>merge</sub>                                  | 0.119 (1.924)                       |
| <i>R</i> <sub>p.i.m.</sub>                                 | 0.041 (0.779)                       |
| Overall <i>B</i> factor from Wilson plot (Å <sup>2</sup> ) | 25.83                               |

<sup>†</sup> Mean  $I/\sigma(I)$  falls below 2.0 at a resolution of 1.97 Å. CC<sub>1/2</sub> was used to inform resolution cut-off [8].

#### 2.4. Structure Solution and Refinement

The structure of  $\alpha$ -chymotrypsin was solved by molecular replacement using Phaser-MR [9] with chain A of the 4Q2K (with all non-protein atoms removed) as the search model. The final solution contained four copies of the search model in the asymmetric unit, with a translation function Z (TFZ) score of 50.7, and log-likelihood gain (LLG) of 10450. Refinement of atomic coordinates was performed by successive iterations of refinement using phenix.refine [10] and manual rebuilding in Coot [11]. Torsion-angle non-crystallographic symmetry (NCS) restraints were applied. Anisotropic refinement of B-factors was restricted to torsion-liberation-screw (TLS) groups [12]. Both NCS and TLS groups were defined automatically using phenix.refine. Optimization of the relative X-ray/stereochemistry and X-ray/B-factor weights was performed in the final rounds of refinement. Refinement statistics are shown in Table 4. The structure factors and atomic coordinates for the final model were deposited at the Protein Data Bank (PDB) under accession 6DI8. Molecular graphic images were produced using PyMOL (v2.0.7, Schrodinger, LLC, New York City, NY, USA) [13].

Table 4. Structure solution and refinement. Values for the outer shell are given in parentheses.

|  |                            |
|--|----------------------------|
| Resolution range (Å)                       | 28.132–1.859 (1.925–1.859) |
| Completeness (%)                           | 99.81 (99.63)              |
| $\sigma$ cutoff                            | $F > 0.0 \sigma(F)$        |
| No. of reflections, working set            | 93185 (8787)               |
| No. of reflections, test set               | 4889 (468)                 |
| Final <i>R</i> <sub>work</sub>             | 0.1885 (0.3317)            |
| Final <i>R</i> <sub>free</sub>             | 0.2252 (0.3416)            |
| Cruickshank DPI (Å)                        | 0.219                      |
| No. of non-H atoms                         |                            |
| Protein                                    | 7201                       |
| Sulphate ion                               | 65                         |
| Solvent                                    | 1100                       |
| Total                                      | 8366                       |
| R.M.S. deviations                          |                            |
| Bonds (Å)                                  | 0.0059                     |
| Angles (°)                                 | 0.78                       |
| Average <i>B</i> factors (Å <sup>2</sup> ) |                            |
| Protein                                    | 33.1                       |

**Table 4.** Structure solution and refinement. Values for the outer shell are given in parentheses.

|                   |       |
|-------------------|-------|
| Sulphate ion      | 80.2  |
| Water             | 43.6  |
| Ramachandran plot |       |
| Most favoured (%) | 97.45 |
| Allowed (%)       | 2.13  |

### 3. Results and Discussion

The structure of bovine  $\alpha$ -chymotrypsin was solved in space group  $P6_5$  using data to 1.86 Å. The unit cell parameters (Table 3) have not been reported previously for crystals of  $\alpha$ -chymotrypsin with this symmetry, indicating that this is a novel crystal form. Residues 1 to 245 were confidently modelled into the electron density, with the exceptions of Ser14, Arg15, Thr147, and Asn148, which were removed during chymotrypsin activation and autolysis. The final model displays favourable geometric statistics; the only Ramachandran outlier present in each molecule is Ile99 (electron density for Ile99 shown in Figure 1), which forms part of the S2 site and its conformation is well supported by strong electron density. All five disulphide bonds are clearly observed in each subunit. The arrangement of subunits is such that the N-terminal peptide (residues 1–13) is at the centre of the asymmetric unit, with the active site facing out away from the centre. The asymmetric unit contains an arrangement of four subunits of  $\alpha$ -chymotrypsin exhibiting two-fold non-crystallographic rotational symmetry through three mutually perpendicular axes (Figure 2).

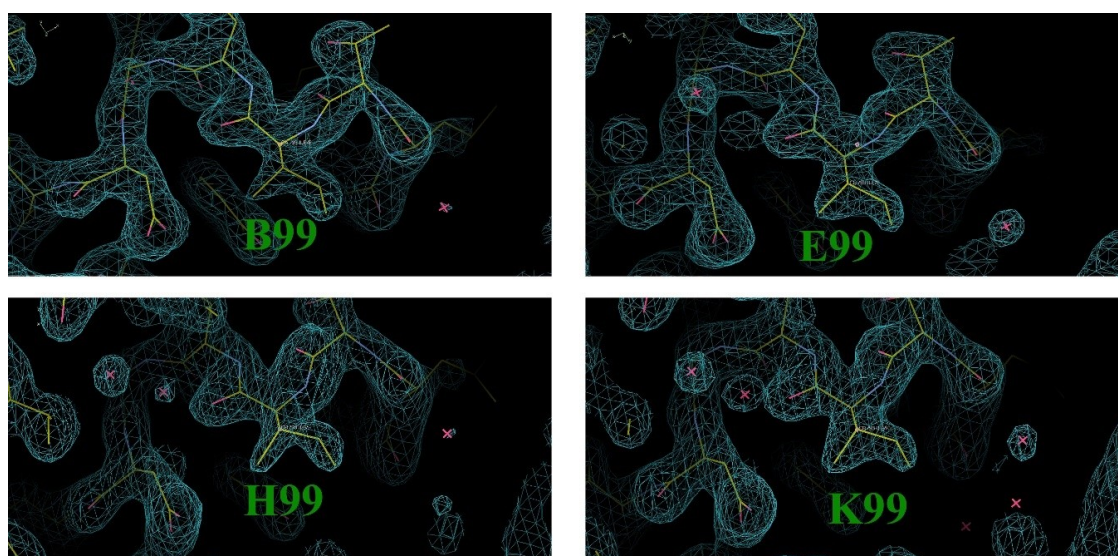


**Figure 1.** Reduced model bias map of residue Ile99 in the chymotrypsin structure solved in space group  $P6_5$ . A composite omit map ( $2F_o - F_c$ , contoured at 1.5  $\sigma$ ) is displayed as blue mesh and proteins are shown as yellow sticks.

Due to this being a new crystal form, the crystallographic interfaces for this  $P6_5$  structure of unliganded  $\alpha$ -chymotrypsin were analysed using PISA (Proteins, Interfaces, Structures and Assemblies) [14] ([http://www.ebi.ac.uk/pdbe/prot\\_int/pistart.html](http://www.ebi.ac.uk/pdbe/prot_int/pistart.html)) and compared to the structure of unliganded  $\alpha$ -chymotrypsin solved in spacegroup  $P2_1$  (PDB ID: 4CHA), which contains two chymotrypsin molecules in the asymmetric unit [15]. Table 5 details the interfaces for  $\alpha$ -chymotrypsin solved in spacegroup  $P6_5$ . Interfaces for the  $P2_1$  structure are listed in Table S2. Overall, 77% of interface residues for the  $P6_5$  crystal form are at interfaces in the  $P2_1$  structure. Interface 1 is largely conserved in each of the structures, involving 11 hydrogen bonds and 1 salt bridge, and is formed between molecules of the asymmetric unit of the  $P2_1$  structure, but between symmetry-mates of our  $P6_5$  crystal (Figure 3). This is the dimerization interface of  $\alpha$ -chymotrypsin, which is formed by the active

site face of each monomer [15,16]. Thus, the tetramer asymmetric unit observed in  $P6_5$  contains four subunits; each individual subunit forms a biological assembly (dimer) with crystallographic symmetry mates. Interface 2 also consists of the same residues for the  $P6_5$  and  $P2_1$  forms. Multiple bonding interactions are observed at this interface for the  $P6_5$  crystal form, with 10 hydrogen bonds and 2 salt bridges identified. For the  $P2_1$  crystal form, however, only a single salt bridge is present. This is consistent with tighter packing at the central interfaces of the  $P6_5$  crystal form. Although most of the residues involved in interface formation are shared between these structures, interfaces 3–6 were not conserved, due to the evident difference in crystal packing. The residues forming each of these interfaces in space group  $P6_5$  were shared across several interfaces of the  $P2_1$  crystal form.

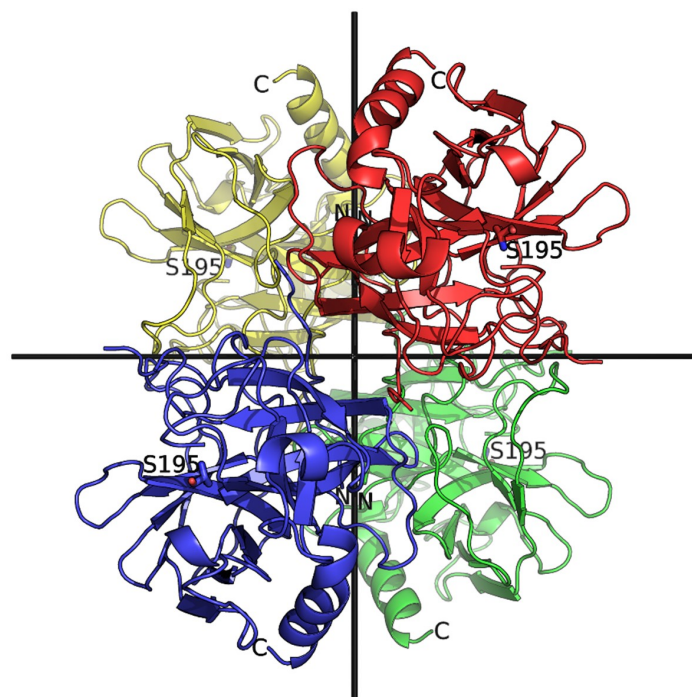


**Figure 2.** Asymmetric unit of bovine  $\alpha$ -chymotrypsin crystallized in space group  $P6_5$  (PDB ID: 6DI8). The four chymotrypsin molecules are coloured differently and shown in cartoon representation. The view is down one axis of two-fold non-crystallographic symmetry; the other two perpendicular axes are shown as black bars. The nucleophilic serines (Ser195) at the catalytic site are shown as sticks. N- and C-termini are labelled.

**Table 5.** Crystallographic interfaces for unliganded  $\alpha$ -chymotrypsin in space group  $P6_5$ .

| Interface # | Symmetry Operation | Interface Area ( $\text{\AA}^2$ ) | Subunits <sup>†</sup> |
|-------------|--------------------|-----------------------------------|-----------------------|
| 1           | X-Y, X+1, Z-1/6    | 1049                              | B, C                  |
|             | X-Y, X, Z-1/6      | 1038                              | A, D                  |
| 2           | X, Y, Z            | 668                               | D, B                  |
|             | X, Y, Z            | 625                               | C, A                  |
| 3           | X, Y, Z            | 562                               | D, A                  |
|             | X, Y, Z            | 539                               | C, B                  |
| 4           | X, Y, Z            | 344                               | B, A                  |
|             | X, Y, Z            | 340                               | D, C                  |
| 5           | -X-1, -Y, Z-1/2    | 361                               | A, C                  |
|             | -X-1, -Y, Z-1/2    | 218                               | B, D                  |
| 6           | -X-1, -Y, Z-1/2    | 145                               | A, D                  |
|             | -X-1, -Y, Z-1/2    | 136                               | B, C                  |

<sup>†</sup> Subunits A–D constitute the asymmetric unit. Each subunit is composed of three separate polypeptide chains, crosslinked by disulphide bonds.



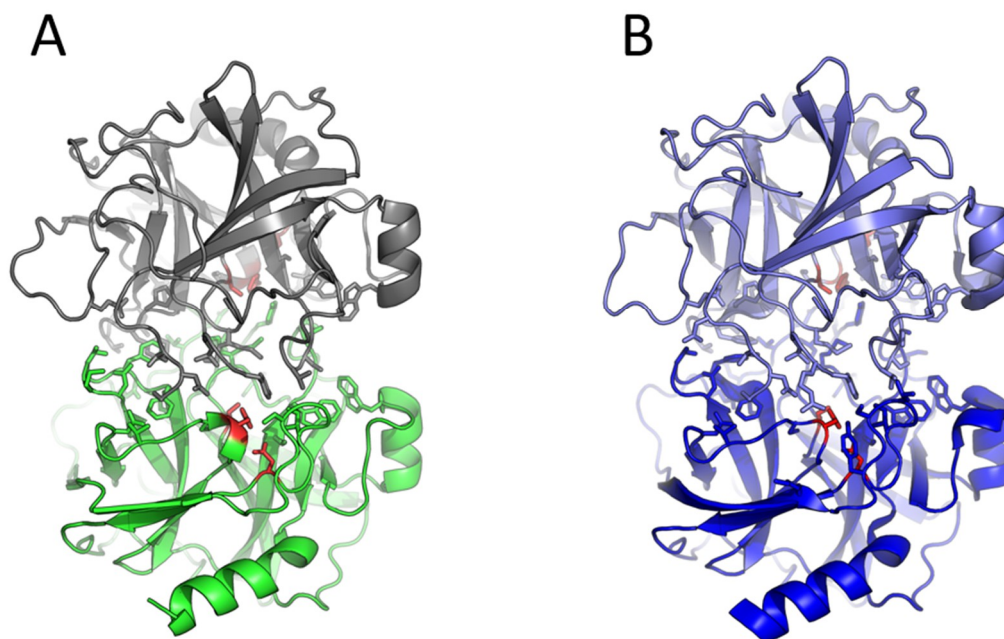


**Figure 3.** The major interface (“interface 1”—see text) present in the crystal lattice is conserved between  $\alpha$ -chymotrypsin crystallized in space group  $P6_5$  and in  $P2_1$ . **(A)** A single chymotrypsin molecule of the asymmetric unit of the  $P6_5$  crystal form is shown in cartoon representation coloured green; the symmetry mate is coloured grey. Interfacing residues are shown as sticks; catalytic residues (His57, Asp102 and Ser195) are coloured red. **(B)** The asymmetric unit of  $\alpha$ -chymotrypsin crystallized in  $P2_1$  (PDB ID: 4CHA).

It has been reported previously that changes in pH can affect the crystal form of  $\alpha$ -chymotrypsin [17,18]. It is possible that the observed differences in crystal packing are due to the higher pH for the  $P6_5$  crystal form, being crystallized at pH 7.0, compared to pH 4.2 for the  $P2_1$  crystal form.

**Supplementary Materials:** The following are available online at <http://www.mdpi.com/2073-4352/8/12/460/s1>, Table S1: Summary of space groups and unit cell parameters for representative bovine  $\alpha$ -chymotrypsin crystal structures currently deposited at the PDB, Table S2: Crystallographic interfaces with areas greater than 100 Å<sup>2</sup> for unliganded bovine  $\alpha$ -chymotrypsin in space group  $P2_1$  (PDB: 4CHA).

**Author Contributions:** Conceptualization, J.B. and A.A.; methodology, B.K.; software, A.M.; validation, A.M., J.P., and J.B.; formal analysis, J.P. and A.M.; investigation, B.K. and A.M.; resources, J.B. and A.M.; data curation, A.M.; writing—original draft preparation, A.M., J.P., and J.B.; writing—review and editing, A.M., J.P., and J.B.; visualization, A.M., J.P., and J.B.; supervision, J.B. and A.A.; project administration, J.B. and A.A.; funding acquisition, A.A.

**Funding:** This research was funded by the Australian Research Council (CE140100003).

**Acknowledgments:** This research was undertaken on the MX1 beamline at the Australian Synchrotron, part of ANSTO.

**Conflicts of Interest:** The authors declare no conflict of interest. The funders had no role in the design of the study; in the collection, analyses, or interpretation of data; in the writing of the manuscript, or in the decision to publish the results.

## References

1. Sharma, S.K.; Hopkins, T.R. Activation of bovine chymotrypsinogen-A - isolation and characterization of mu-chymotrypsin and omega-chymotrypsin. *Biochemistry* **1979**, *18*, 1008–1013. [[CrossRef](#)] [[PubMed](#)]
2. Matthews, B.W.; Sigler, P.B.; Henderson, R.; Blow, D.M. 3-dimensional structure of tosyl-alpha-chymotrypsin. *Nature* **1967**, *214*, 652–656. [[CrossRef](#)] [[PubMed](#)]

3. Chua, K.C.; Pietsch, M.; Zhang, X.; Hautmann, S.; Chan, H.Y.; Bruning, J.B.; Gutschow, M.; Abell, A.D. Macrocyclic protease inhibitors with reduced peptide character. *Angew. Chem. Int. Ed. Engl.* **2014**, *53*, 7828–7831. [[CrossRef](#)] [[PubMed](#)]
4. Roussel, A.; Mathieu, M.; Dobbs, A.; Luu, B.; Cambillau, C.; Kellenberger, C. Complexation of two proteic insect inhibitors to the active site of chymotrypsin suggests decoupled roles for binding and selectivity. *J. Biol. Chem.* **2001**, *276*, 38893–38898. [[CrossRef](#)] [[PubMed](#)]
5. Neidhart, D.; Wei, Y.; Cassidy, C.; Lin, J.; Cleland, W.W.; Frey, P.A. Correlation of low-barrier hydrogen bonding and oxyanion binding in transition state analogue complexes of chymotrypsin. *Biochemistry* **2001**, *40*, 2439–2447. [[CrossRef](#)] [[PubMed](#)]
6. McPhillips, T.M.; McPhillips, S.E.; Chiu, H.J.; Cohen, A.E.; Deacon, A.M.; Ellis, P.J.; Garman, E.; Gonzalez, A.; Sauter, N.K.; Phizackerley, R.P.; et al. Blu-Ice and the Distributed Control System: software for data acquisition and instrument control at macromolecular crystallography beamlines. *J. Synchrotron Radiat.* **2002**, *9*, 401–406. [[CrossRef](#)] [[PubMed](#)]
7. Leslie, A.G.W.; Powell, H.R. Processing Diffraction Data with Mosflm. In *Evolving Methods for Macromolecular Crystallography*; Read, R.J., Sussman, J.L., Eds.; Springer: Dordrecht, The Netherlands, 2007; Volume 245, pp. 41–51.
8. Karplus, P.A.; Diederichs, K. Assessing and maximizing data quality in macromolecular crystallography. *Curr. Opin. Struct. Biol.* **2015**, *34*, 60–68. [[CrossRef](#)] [[PubMed](#)]
9. McCoy, A.J.; Grosse-Kunstleve, R.W.; Adams, P.D.; Winn, M.D.; Storoni, L.C.; Read, R.J. Phaser crystallographic software. *J. Appl. Crystallogr.* **2007**, *40*, 658–674. [[CrossRef](#)] [[PubMed](#)]
10. Afonine, P.V.; Grosse-Kunstleve, R.W.; Echols, N.; Headd, J.J.; Moriarty, N.W.; Mustyakimov, M.; Terwilliger, T.C.; Urzhumtsev, A.; Zwart, P.H.; Adams, P.D. Towards automated crystallographic structure refinement with phenix.refine. *Acta Crystallogr. D Biol. Crystallogr.* **2012**, *68*, 352–367. [[CrossRef](#)] [[PubMed](#)]
11. Emsley, P.; Lohkamp, B.; Scott, W.G.; Cowtan, K. Features and development of Coot. *Acta Crystallogr. D Biol. Crystallogr.* **2010**, *66*, 486–501. [[CrossRef](#)] [[PubMed](#)]
12. Winn, M.D.; Isupov, M.N.; Murshudov, G.N. Use of TLS parameters to model anisotropic displacements in macromolecular refinement. *Acta Crystallogr. D Biol. Crystallogr.* **2001**, *57*, 122–133. [[CrossRef](#)] [[PubMed](#)]
13. Schrodinger, LLC. The PyMOL Molecular Graphics System, Version 1.8. 2015.
14. Krissinel, E.; Henrick, K. Inference of macromolecular assemblies from crystalline state. *J. Mol. Biol.* **2007**, *372*, 774–797. [[CrossRef](#)] [[PubMed](#)]
15. Tsukada, H.; Blow, D.M. Structure of alpha-chymotrypsin refined at 1.68 Å resolution. *J. Mol. Biol.* **1985**, *184*, 703–711. [[CrossRef](#)]
16. Ikeda, K.; Kunugi, S.; Ise, N. pH dependence of the formation of dimeric alpha-chymotrypsin and its catalytic activity. *J. Biochem.* **1982**, *92*, 541–546. [[CrossRef](#)] [[PubMed](#)]
17. Corey, R.B.; Battfay, O.; Brueckner, D.A.; Mar, F.G. Preliminary X-ray diffraction studies of crystal forms of free and inhibited chymotrypsin. *Biochim. Biophys. Acta* **1965**, *94*, 535–545. [[CrossRef](#)]
18. Vandlen, R.L.; Tulinsky, A. Changes in the tertiary structure of alpha-chymotrypsin with change in pH: p4 4.2–6.7. *Biochemistry* **1973**, *12*, 4193–4200. [[CrossRef](#)] [[PubMed](#)]

